



Integration of Electric Vehicles in the Unit Commitment Problem with Uncertain Renewable Electricity Generation

Panagiotis Adraktas, Athanasios Dagoumas*

Department of International and European Studies, Energy and Environmental Policy Laboratory, University of Piraeus, PC 18532 Piraeus, Greece. *Email: dagoumas@unipi.gr

Received: 17 September 2018

Accepted: 02 January 2019

DOI: <https://doi.org/10.32479/ijeeep.7125>

ABSTRACT

The integration of electric vehicles (EVs) in the power system is a challenging issue for the power system and network operators. The paper uses several Unit Commitments (UC) models which incorporate high levels of wind power production, applying different methods to tackle the renewables' uncertainty. The selected power system is IEEE RTS 96. The UC models are further extended to integrate the EVs. Our focus is to assess the EVs impact on the total operating cost and the power grid adequacy to handle the extra load, by examining different charging profiles and penetration levels of EVs with the different UC models. Simulation results show that an optimized charging strategy is considerably more efficient than the random charging strategy, both in the total operating cost and the ability to integrate more EVs. The comparison between the UC models show that the most robust UC model leads to higher total operating cost, due to its more conservative methodology to tackle the stochastic nature of wind. There exists a non-linear trade-off between power system robustness and the total operating cost, depending on each power system characteristics, affecting also the penetration level of EVs.

Keywords: Electric Vehicles, Unit Commitment, Renewables, Uncertainty, Power System, IEEE RTS 96

JEL Classifications: Q47, L94

1. INTRODUCTION

Electric vehicles (EVs) are a promising technology for drastically reducing the environmental burden of road transport, especially within the urban areas. In the EU, a percentage of 73% of all oil is consumed by the transport sector (CIGRE, 2015). The competition among car manufacturers is strong, facilitating the earlier penetration of EVs than initial forecasts (Kampman et al., 2011). The introduction of a vast number of EVs in modern power systems will affect a wide variety of factors in the operation of power systems and markets of electricity. First of all, the power systems and the distribution networks will be loaded with extra power during the peak hours (Grahn, 2013). That will create the need for additional power production capacity available, as well as for more capacity available both for the transfer and the distribution networks (Clement-Nyons et al., 2009). Another crucial

factor is the stability of the system which will be highly affected by both the stochastic production of the renewable sources and the stochastic charging of the EVs. Finally, the prices of electricity will be affected, depending on the ways that will be decided to produce the extra energy that will cover the electrified mobility demand (Schill and Gerbaulet, 2015). Last but not least, we should consider the impact of the additional power generation on the environment. Studies have indicated that if the electricity is produced by "dirty" power plants, then the reduction of gas emissions is negligible, making thus the electrification of road transports an ineffective measure for gas emissions reduction (Kasten et al., 2016). Another potential is the use of fleets of electric-drive vehicles for grid support (Tomic and Kempton, 2007). A greater penetration of renewable sources combined with EVs will lead to a reduction of gas emissions from the transport sector (Willett and Jasna, 2005; Mariasiu, 2012). Secondly, the investments on production

capacity and transfer/distribution capacity could be reduced with the introduction of smart charging technologies and Vehicle to Grid services. Thirdly, big parking lots could be used as Load aggregators who could provide ancillary services for the systems during peak hours, something that could further lead to a reduction in the usage cost for the vehicle owner (Boumis, 2012).

The integration of EVs in the power system stands a challenging issue for the power system and network operators. It is a complex issue which requires detailed and robust methodologies to quantify their effects on the power system. The aim of a Unit Commitment (UC) algorithm is to determine which units will produce energy each hour of a day to meet the demand. The UC problem is complex, as it incorporates several techno-economic constraints related to the production units and the transmission lines. The UC problem identifies the power units' dispatch considering their operational and maintenance costs, their ramping capacity, their capability to provide ancillary services and other techno-economic criteria. The UC problem is formulated as a Mixed Integer Linear Programming problem, which is adequate to handle such complicated problems. The problem is solved in a way that the overall fuel cost is minimized in respect with the system's and unit's constraints.

The integration of EVs in the UC problem is expanding rapidly over the last years. Yang et al. (2017) provide a comprehensive study of economic UC of power systems integrating various renewable generations and plug-in EVs (PEV). The paper considers four different cases of UC problems with various weather and season scenarios using real power system data are conducted and solved, and smart management of charging and discharging of PEVs are incorporated into the problem. Test results confirm the efficacy of the proposed framework. Tafreshi et al. (2016), develop a probabilistic UC model for optimal operation of PEVs in microgrid. The microgrid is made up of microturbines, wind turbine, boiler, PEVs, thermal storage and battery storage. The probabilistic UC optimizes the objective function using Particle Swarm Optimization algorithm, comparing it with a simple deterministic model. Koltsaklis and Georgiadis (2016) present an integrated UC model incorporating EVs as a flexible and responsive load. The model is applied in the Greek power system.

Talebizadeh et al. (2014) provide an evaluation of PEVs impact on cost-based UC. The paper proposes charging and discharging schedule of PEVs with respect to load curve variations. The proposed methodology incorporates integrated parking lots into the UC problem. The model is applied on the IEEE 10-unit test system showing a significant techno-economic saving. Zhang et al. (2015) develop a fuzzy chance-constrained program for UC problem considering demand response, EV and wind power. The paper uses a fuzzy chance-constrained program that takes into account the wind power forecasting errors. The numerical study shows that the model can promote the utilization of wind power evidently, making the power system operation more eco-friendly and economical. Wang et al. (2015) present an efficient power plant model of EVs for UC of large-scale wind farms. Zhou et al. (2016) provide a power system steady-state analysis with large-scale EV integration. The paper establishes a model framework

which examines, using United Kingdom power system data, four major issues: EV capacity forecasting, optimization of an object function, EV station siting/sizing and steady-state stability. The proposed model is used to establish criteria for EV station siting and sizing and to determine steady-state stability using a real model of a small-scale city power system.

Villar et al. (2016) examine the combined penetration of wind and solar generation with PEVs. This paper used a UC model for the Spanish power system, providing some insight on how the penetration of these technologies affects relevant variables such as energy and reserve, thermal plants behaviour and systems costs. Results show that PEV increase total demand, but its optimal charging smooth's the net demand and the final electricity prices. Heydarian-Forushani et al. (2016) focus on the flexible interaction of PEV parking lots for efficient wind integration. The paper proposes a two-stage stochastic programming market-clearing model considering the network constraints to achieve the optimal scheduling of conventional units as well as PEVs' parking lots in providing both energy and reserve services. It demonstrates that coordinated operation of parking lots can facilitate wind power integration. Hanemann et al. (2017) provide insights on the effects of EV charging strategies on the German power system. The paper finds that curtailment of renewable energy sources is reduced independently of the charging strategy, while the charging strategy vehicle-to-grid proves to be most beneficial concerning system cost and emissions. Haque et al. (2016) present a dispatch model integrating wind generators and EVs. The proposed model aims to utilize the flexibility of fleets of PEVs to optimally compensate for the wind generation uncertainty. Effects of smart charging on generation cost, CO₂ emissions and total network load are assessed.

Ul-Haq et al. (2018) developed a probabilistic model, concerning the EV charging patterns within a residential distribution network. The stochastic model provides rigorous estimation of EVs charging pattern. Mkahl et al. (2017) examined the charging management of EVs fleets and developed an optimum algorithm. The authors examine both normal conditions, such as driving without using electrical accessories, roads without traffic jams and stops, as well as disturbed conditions. Karfopoulos and Hatzigiorgiou (2017) propose a bidirectional EV coordination algorithm for conforming to an energy schedule, implementing the Bender Decomposition method to define EVs' optimal response to the aggregator's pricing policy. Baringo and Amaro (2017) develop a stochastic robust optimization model to simulate the bidding strategy of an EV aggregator, leading to reduced charging costs without affecting the driving requirements of EV users. Bharati and Paudyal (2016) implement optimal hierarchical framework for EVs integration in the distribution grid, which leads to reduced cost of EVs charging and reduced power losses in the distribution grid.

The literature review shows that there is a rapidly growing research on the integration of EVs in the power systems. There are several research papers aiming at the optimum integration of EVs, through the adoption or incentivizing of different charging methods. There also several papers on examining the impact of EVs on the distribution grid, focusing on the technical aspects, such as reliability issues and the provision of ancillary services.

The consideration of UC models is also extended, as they are considered robust approaches to simulate the power systems operation. There are several UC models used for examining the impact of EVs, in relationship or not of the penetration of renewable energy resources. However, UC models examine - in most cases - a national power system or a small power system, providing insights on the effect of EVs on it. Moreover, there are few cases providing a comparison among different UC models, towards revealing the required level of detail for robust solutions and the impact of uncertainties on key variables. The Energy and Environmental Policy laboratory at the University of Piraeus has extensive experience in the developing and extending UC models, which however mainly concerns the Hellenic power system (Dagoumas and Polemis, 2017; Dagoumas et al., 2017; Koltsaklis et al., 2017; Dagoumas and Koltsaklis, 2017; Koltsaklis and Dagoumas, 2018). Considering that the integration of EVs is a challenging issue, the application of a common power system such as the IEEE RTS 96 with increased penetration of renewables has been selected, as this represents a large but as well a more commonly used power system in the international community. This has led to application and extension of UC models by the Renewables Energy Analysis Lab at the University of Washington (REAL, 2017).

The paper contributes to the literature by applying different UC models, differentiated by the approach tackling uncertain renewable electricity generation, to estimate the impact of integrating EVs, by examining different charging profiles and penetration levels of EVs in a commonly used power system. The highlights of the paper are: (i) Integration of EV in the UC problem, (ii) comparison of different UC models on the IEEE RTS 96 power system, tackling differently the uncertainty of renewable electricity generation, (iii) implementation of different charging profiles to evaluate the impact of the EVs' load and (iv) provision of useful insights into the effects of the EVs' load on the total operating cost of a power system and its adequacy to handle the excessive load under different charging strategies.

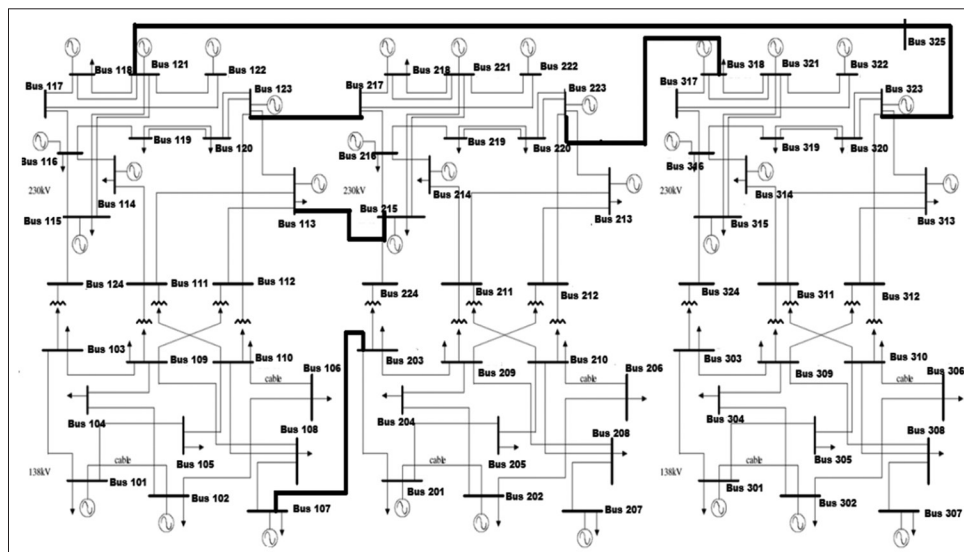
The rest of the paper is organized: Sections 2 provide the formulation of the models. Section 3 provides the case study where the models are applied, while Section 4 provides the results and a relevant discussion on them. Finally, section 5 provides the main conclusions and highlights of the paper.

2. MATHEMATICAL FORMULATION

The Renewables Energy Analysis Lab at the University of Washington has developed five different implementations of the UC problem (Pandzic et al., 2017), where the basic formulation is described in Annex I. The application of the UC models concerns the IEEE RTS-96 power system, shown in Figure 1. This power system includes, apart from thermal production units of various fuel (nuclear, coal-fired, diesel, natural gas), renewable energy generation units from the wind, which power production is uncertain compared to other renewable technologies, such as photovoltaics. Specifically, there are 19 wind power plants of total wind production capacity of 6900 MW. The wind power plants are distributed in the following way: 3900 MW in the West subsystem, 2400 MW in the central subsystem and 600 MW in the east subsystem. There are also 73 buses, 120 transmission lines, 96 thermal power units and 51 loads. The whole system can be seen in the following layout.

The inclusion of renewable energy sources in a power system introduces uncertainty on the real production of those units. The uncertainty comes from the stochastic nature of the wind and the weather conditions in general. Transmission system operators have to forecast the real output from those renewable sources to calculate the thermal power needed to meet the electricity demand and ensure the system stability. The stochastic wind power production is a major parameter in the system instability, and the high penetration of renewable production must be compensated with the installation of flexible thermal production units or hydropower, which can increase and decrease their output rapidly. As a matter of fact, the forecasting of the renewable energy sources real output is a major problem for the transmission system

Figure 1: The electrical system IEEE RTS-96



operators. It affects the stability of the power system and the energy market participants as well as the energy markets itself. We did not consider other renewable technologies, such as photovoltaics as their power output can be forecasted with much higher accuracy, so practically the introduction of photovoltaics would lead to an upgrade of the net load at each bus, rather than an introduction of uncertain renewables production. Photovoltaics, besides the case of the sunset effect, which affects the UC problem and enhances the need for flexible ramping capacity, it does not inherit uncertainty in the dispatch of power units, as the uncertain power output from the wind farms is doing.

The models developed by the Renewables Energy Analysis Lab, that used for this paper are the following: Deterministic UC (DUC), Stochastic UC (SUC), Improved interval UC (IIUC), IUC and Robust UC (RUC). Each of those models uses a different mathematical procedure to forecast the anticipated renewable production. Some of them are more preservative than the others. Consequently, it is committing more thermal units, and the stability of the system is increased but with a higher total economic cost. The UC models require a considerable amount of input data, which are described the model developers’ website (REAL, 2017). The models’ users have the option to change some options, i.e., to modify the penetration of the renewable sources, the variable cost, and ramping capabilities of thermal units, the capacities of the transmission lines, the wind profile and a penalty factor in the case of spilled wind production or unserved loads. In our research, we choose to have 30% of energy from wind power units, which is much higher than the current state of most power grids and a possible future power system of the next decades. Another decision is to go with the unfavourable or favourable wind profile. We have chosen the unfavourable wind profile, as depicted in Figure 2.

2.1. UC Models

In our analysis we have used the following REAL UC models, aiming to compare the different way the uncertainty of wind is tackled:

- DUC model
- SUC model
- IUC model

- IIUC model
- RUC model.

Considering the theoretical model differences, a recent work (Kirschen, 2014) confirms those results. Figure 3 summarizes the differences between the different models. Figure 3 shows that more RUC models, being more “conservative” in constraints, lead to the commitment of more power from dispatching units. We have extended the models to incorporate the EVs as described in section 3.

3. EVS

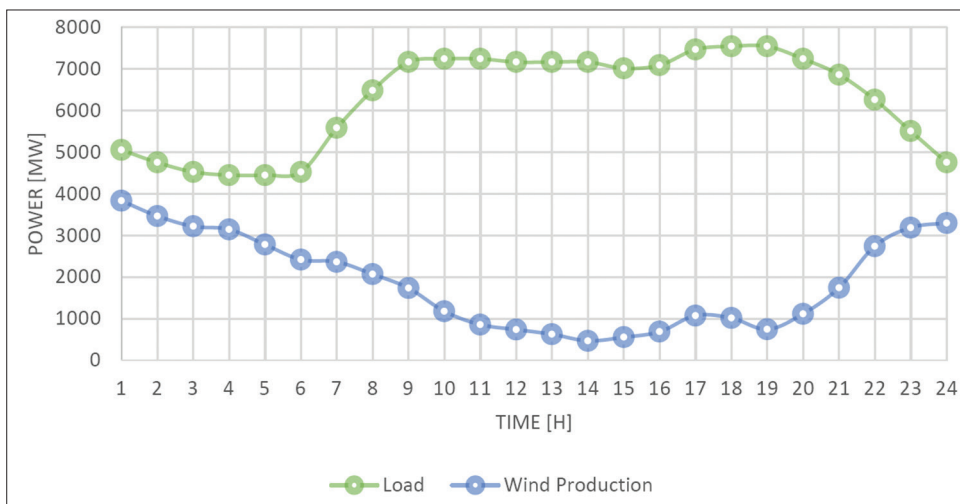
3.1. Number of EVs

In developed countries, such as the US, Germany, Japan, France, Italy, the yearly electricity production per capita ranges between 5000 kWh/cap and 12000 kWh/cap, as shown in Table 1. Thus, we derive that an average of about 8500kWh/cap will be used for our calculations, which means that we have an average of 1kW/cap of annual power level. The examined power system consists of 10215MW of thermal energy production capacity, which means that this power system is the equivalent system for a population of 10.215 million people. According to Eurostat (2017) in 2014 in EU, there were on average around 0.45 cars/capita, as shown in Table 2. As a result, in the examined power system, there could be 4,596,750 EVs if we had a 100% penetration of Evs.

3.1.1. Battery capacity and charging

There are two categories of EVs; the plugin hybrids and the fully EVs. In the first category, the battery capacity used varies from 4.4 kWh to 17 kWh, for example, Toyota Prius III (plug-in hybrid) encapsulates 9 kWh and can be charged with a 3.3 kW charger, whereas the Chevrolet Volt engages an 18 kWh battery and can be charged with a 3.6 kW charger. The second category is the fully EVs where someone finds capacities between 19 and 100 kWh (Plugincars, 2017), as shown in Table 3. The current research assumes that only fully EVs will be used and thus it is decided to proceed with a 35 kWh battery capacity for all the vehicles to be able to complete all the daily journeys on one battery charge.

Figure 2: Load profile and wind production profile



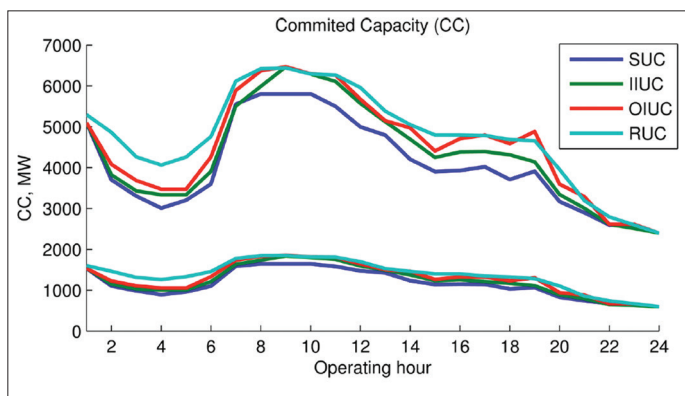
Source: REAL, 2017

Table 1: Consumption of electricity in developed countries

| Country | Population | Electricity consumption (kWh) | Electricity consumption/cap (kWh) |
|-------------|------------|-------------------------------|-----------------------------------|
| EU | 513949445 | 2.771E+12 | 5446 |
| USA | 323995528 | 3.913E+12 | 12199 |
| Japan | 126702133 | 9.34E+11 | 7446 |
| Germany | 80722792 | 5.33E+11 | 6669 |
| France | 66836154 | 4.31E+11 | 6513 |
| UK | 64430428 | 3.09E+11 | 4844 |
| Italy | 62007540 | 2.91E+11 | 4740 |
| Canada | 35362905 | 5.28E+11 | 15081 |
| Belgium | 11409077 | 8.1E+10 | 7171 |
| Greece | 10773253 | 5.3E+10 | 4969 |
| Sweden | 9880604 | 1.27E+11 | 12983 |
| Austria | 8711770 | 6.975E+10 | 8087 |
| Switzerland | 8179294 | 5.8E+10 | 7162 |
| Denmark | 5593785 | 3.2E+10 | 5778 |
| Finland | 5498211 | 8.1E+10 | 14880 |
| Average | | | 8265 |

Source: CIA, 2017

Figure 3: Committed capacity using different UC models and different wind profile (favourable for the upper group of lines and unfavourable for the lower group of values)



Source: Kirschen, 2014

According to the commercially available models, the consumption of electricity varies between 0.12 and 0.20 kWh/km. We assume 0.175 kWh/km as an average value that represents most of the models of Table 3. There are different charging options available according to the limits of the power lines. This thesis assumes that a 3kW charger will be used for vehicles running journeys up to 80km and another type of “fast charger” at 6kW maximum charging capacity will be used for vehicles running longer journeys and should be charged before the next morning in a period of 5-6 h. The assumptions concerning the driving patterns are provided in Annex III.

3.2. Integration of EVs in the UC Models

Using the above information and a recent work (Madzharov et al., 2014) as a base, we develop an algorithm, which will integrate all the EVs data into the UC. We assume that because the data comes from well-developed countries such as the United Kingdom and Sweden should represent a good traveling model for European Union countries and other developed countries. During night hours (23.00-05.00) we observe a tiny percentage of trips, either one-way or two-way. Thus, we assume that during these hours no trips are taking place and therefore, we

Table 2: Cars per capita

| Country | Cars/capita |
|---------------|-------------|
| Belgium | 0.496 |
| Bulgaria | 0.416 |
| CzechRepublic | 0.448 |
| Germany | 0.550 |
| Estonia | 0.496 |
| Ireland | 0.438 |
| Greece | 0.468 |
| Spain | 0.471 |
| France | 0.483 |
| Croatia | 0.347 |
| Italy | 0.610 |
| Cyprus | 0.558 |
| Latvia | 0.329 |
| Lithuania | 0.410 |
| Hungary | 0.315 |
| Malta | 0.625 |
| Netherlands | 0.473 |
| Austria | 0.552 |
| Poland | 0.526 |
| Portugal | 0.451 |
| Romania | 0.246 |
| Slovenia | 0.518 |
| Slovakia | 0.360 |
| Finland | 0.582 |
| Sweden | 0.475 |
| UK | 0.452 |
| Liechtenstein | 0.767 |
| Norway | 0.500 |
| Switzerland | 0.539 |
| Turkey | 0.129 |

Source: Eurostat, 2017

distribute these few percentages into the rest time periods. The derived allocation of journeys starting hours is in the Table 4.

The main purpose of the algorithm is to charge all the vehicles’ batteries into a 24 h horizon day. For example, if a car starts its journey at 6.00 it should be charged by then, but if it starts at 10.00, then it should be charged by 9.00. To this respect, we want in a 24 h’ period to charge the electric consumption of the EVs. The reason why we did not use strict constraints on the charging time is explained by the large number of vehicles that we will

Table 3: Commercially available electric vehicles and their characteristics

| Electric vehicle model | Battery capacity (kWh) | Charger (kW) | Battery range (km) | Electricity consumption (kWh/km) |
|------------------------|------------------------|--------------|--------------------|----------------------------------|
| BMW i3 | 33 | 7.7 | 183 | 0.1799 |
| Chevrolet bolt | 60 | 7.2 | 383 | 0.1566 |
| Chevrolet Spark EV | 19 | 3.3 | 132 | 0.1440 |
| Volkswagen E Golf | 24 | 7.2 | 134 | 0.1797 |
| Ford focus electric | 23 | 6.6 | 185 | 0.1243 |
| Nissan leaf | 30 | 6.6 | 172 | 0.1742 |
| TeslaModel S | 100 | 10 | 507 | 0.1973 |

use. Consequently, we assume an equal distribution of the 24 h. Another critical assumption that will be utilized is that due to the size of the electric system, we will equally distribute the number of electric cars on each bus bar and we will further assume that each EV will always be charged on the same bus bar.

It is important to clarify how the two-way and one-way trips are calculated. A trip in the one-way category is made at once for example at 40 km. However, an EV in the two-way category makes two trips at 20 km each, therefore in total 40 km/day. The most important number that should be derived from the previous data to perform the desired calculations is the number of EVs that start their journeys each hour.

The total number of EVs in the system, at 100% penetration level, ($EV_{p100\%}$) is the sum of the number of EVs that make one trip (EV_{one}) and the number of EVs that make two trips (EV_{two}) per day:

$$EV_{p100\%} = EV_{one} + EV_{two} \tag{1}$$

The number of trips in the one-way group is equal to the number of EVs in that group:

$$Trips_{one} = EV_{one} \tag{2}$$

The total number of trips in the two-way group is twice the number of EVs in that group:

$$Trips_{two} = 2 \times EV_{two} \tag{3}$$

The total number of trips is equal to the sum of the one-way and two-way group:

$$Trips_{total} = Trips_{one} + Trips_{two} \tag{4}$$

In the previous paragraph, we calculated that the one-way trips are 5% of the total trips the factor that represents this figure will be from now on called f_1 . Then:

$$Trips_{one} = f_1 \times Trips_{total} \tag{5}$$

By substituting equations (3) and (4) into equation (5):

$$Trips_{total} = EV_{one} + 2 \times EV_{two} \tag{6}$$

By substituting equations (2) and (7) into equation (6):

$$EV_{one} = f_1 \times (EV_{one} + 2 \times EV_{two}) \tag{7}$$

Table 4: Percentage of trips starting during each period over a 24-h horizon

| h | One-way (%) | Two-way (%) |
|-----|-------------|-------------|
| t1 | 0.00 | 0.00 |
| t2 | 0.00 | 0.00 |
| t3 | 0.00 | 0.00 |
| t4 | 0.00 | 0.00 |
| t5 | 0.00 | 0.00 |
| t6 | 0.01 | 1.50 |
| t7 | 0.08 | 5.10 |
| t8 | 0.17 | 10.20 |
| t9 | 0.25 | 6.50 |
| t10 | 0.40 | 4.70 |
| t11 | 0.59 | 5.50 |
| t12 | 0.40 | 5.70 |
| t13 | 0.40 | 6.40 |
| t14 | 0.40 | 5.90 |
| t15 | 0.50 | 6.70 |
| t16 | 0.40 | 7.40 |
| t17 | 0.40 | 9.70 |
| t18 | 0.25 | 7.30 |
| t19 | 0.25 | 5.10 |
| t20 | 0.17 | 2.80 |
| t21 | 0.17 | 2.20 |
| t22 | 0.08 | 1.50 |
| t23 | 0.08 | 0.80 |
| t24 | 0.00 | 0.00 |
| Sum | 5.00 | 95.00 |

By combining equations (2) and (8), we calculate the number of EVs in the two-way group and then by using that result and equation (2) we extract the number of EVs in the one-way group. Finally, by using these results, we calculate the total trips using only the $EV_{p100\%}$ and f_1 .

After $Trips_{total}$ is calculated we use the distributions presented in Annex III to determine the number of EVs starting each hour and how many kilometers each group of EVs runs.

Knowing the number of total trips $Trips_{total}$, the number of trips started each hour and the distance that each group of EVs runs; we can now derive the number of parked EVs in each cluster that is connected to the grid and ready to be charged and their battery capacities $EVs_{Available}(e,t)$. Also, the energy that is consumed by the $EVs_{ConsumedEnergy}(e,t)$ is calculated. These parameters are now used in the optimization of the UC models.

3.3. UC Model Extension for the Integration of EVs

In the previously described formulation for the UC model, we will make a few additions to the model to take into

account the extra load coming from the EVs that will be charging. The additions that we should make are at two levels: Firstly, we should update the excel input file so that the values for the new parameters are introduced to the UC model. Secondly, we should add the new equations and constraints that model the EV load as described before. In this section, we describe the formulation added to UC models to integrate a flexible load from EVs.

3.3.1. Nomenclature

A. Indices

E = Index of same distance traveling EVs group 1-E

B. Parameters

$Trips_{es}$ = Trips started each hour per EV distance group e and bus bars

$EVsAvailable_{es}$ = EVs that are available for charging each hour

$Consumption_e$ = Energy consumption per EVs group e

$BatteryFull_e$ = Total battery capacity of all cars for each group e

$ChargeLine_e$ = Power of the charger that each group of EVs can be charged by (MW)

$MaxTransfer_{es}$ = Maximum charging load each hour according to the EvsAvailable

C. Variables

$EnergyUp_{es}(t)$ = Additional electricity demand for EVs charging in group e in bus s in hour t (MWh)

$soc_{es}(t)$ = State of charge of EVs in group e in bus s in period t (MWh).

3.3.2. Equations and constraints

Firstly, we have to add in the power balance equation the term that represents the EV charging loads. Then the power balance equation is:

$$\sum_{i=1}^I g_i(t) - \sum_{\{s,m\} \in L/m > s} B_{sm} \cdot (\theta_s(t) - \theta_m(t)) - \sum_{\{s,m\} \in L/m < s} B_{ms} \cdot (\theta_m(t) - \theta_s(t)) = d_s(t) \forall t \leq T, s \leq S, e \leq E \quad (9)$$

Then, we have to calculate the energy consumption for each bus bar for each EV group for each hour.

$$ConsumedEnergy_{es}(t) = Trips_{es}(t) \cdot Consumption_e \forall t \leq T, s \leq S, e \leq E \quad (10)$$

Finally, we have to calculate the state of charge for each group of EVs in each bus s in each period t.

$$soc_{es}(t) = soc_{es}(t-1) + n \cdot EnergyUp_{es}(t) - \frac{1}{n} \cdot ConsumedEnergy_{es}(t) \forall t \leq T, s \leq S, e \leq E \quad (11)$$

The MaxTransfer parameter is calculated manually outside the model via the equation:

$$MexTransfer_{es}(t) = EVsAvailable_{es}(t) \cdot ChargeLine_e(t) \forall t \leq T, s \leq S, e \leq E \quad (12)$$

Finally, we introduce three constraints that ensure that the calculated values will not exceed the appropriate limits.

The first constraint ensures that the charging energy will not be more than the energy needed to top all the batteries.

$$soc_{es}(t-1) + EnergyUp_{es}(t) \leq BatteryFull_{es} \forall t \leq T, s \leq S, e \leq E \quad (13)$$

The following constraint ensures that each hour the charging power will not be more than the maximum output power of the chargers used.

$$EnergyUp_{es}(t) \leq MaxTransfer_{es}(t) \forall t \leq T, s \leq S, e \leq E \quad (14)$$

The last control is that the whole energy that will be used to charge the EVs in each bus bar will be according to the energy that these EVs consumed during the day.

The input data that have been for the integration of EVs in the UC models are provided in Annex III.

4. RESULTS AND DISCUSSION

4.1. Simulation Assumptions

This section provides the results from applying the extended UC models. We have used all above mentioned models, but we choose to present results from three of them: The deterministic, the stochastic and the interval unit UC models, as the results of the robust model are comparable to those of the interval model. The paper examines the effect of the excess load using the UC models, which implement different level of power system robustness. The deterministic model is the easiest to be solved and provides a solution which is based on a static prediction of the wind power generation. However, that prediction relies on statistical data processing of historical data. The stochastic model is using 10 different scenarios of the wind power production forecast. Each scenario is paired with a probability to happen according to its likelihood to occur. However, it is not within the scope of this research to analyze the mathematical methods used to generate the most typical scenarios from the historical data. The interval unit model is much more conservative than the other two, because it commits units to meet the extreme transitions which are extracted from the wind data.

An important issue concerning simulations is the selection of the EVs charging profile. Our research is based on the following three charging profiles, which were used to evaluate the effects of the extra energy demand in the operation of the electric system.

- Optimized charging profile (Profile 1)

In the optimized charge profile, the charging of the EVs is handled by the UC algorithm which is responsible for distributing the additional energy demand across the 24 h to achieve the least total economic cost of the operation of the whole system.

- Random charging profile (Profile 2)

In the random charge profile, the charging of the EVs is done after every trip. That means that if an EV is moving during hour 9, then it will start charging right after its trip at hour 10. It can be derived by combining the statistics used for the driving patterns. According to the driving patterns, all the trips in distance groups up to 6 are being completed within an hour from their beginning. Moreover, only 2.6% of the trips is 160 km and from that only 5% is made at once which means that only 0.13% of the trips last longer than an hour but also <2 h. That means that we will consider the same rule for all the EVs which mean that if a trip starts at hour 9 then its charge will start at hour 10. This profile will test if the energy production capacity of the system is adequate to charge a large number of EVs during the peak hours.

- Off-peak charging profile (Profile 3)

In the off-peak-charge profile, all the EVs can charge only during the off-peak hours, which means that the charging is done during hours 1–8 and 21–24. This charging profile was selected to verify the operation of the UC algorithm and our global assumption that the power system operates better when we do not have big ramps in power demand.

5. RESULTS

5.1. Deterministic Model Results

We have run the deterministic model for the three charging scenarios, and we present the effect on the electricity demand in Annex V. The first and most important result is that the optimized charging profile chooses to allocate the extra electricity demand during the hours that the average demand is low. This action leads to keep the units that would normally be closed, committed to keep up with the standard demand during peak hours. The avoidance of the startup costs will lead to higher efficiency and better use of non-flexible units such as the coal-fired units. The second observation we make is that, as initially assumed, the optimized charging profile has similar results with the off-peak hours charging profile and this is why we expect to have similar total operational costs between those two charging profiles, as confirmed in Figure 4.

If we consider the worst case, when we have 100% penetration of EVs, we can compare the maximum load against the maximum total capacity that is available. In this comparison, it is important to take into account the renewable energy production, representing a considerable amount of 30% of the total daily electric production. To test the power system in challenging situations, we have selected a non-favorable wind profile which provides much power output when the load is low power output when the demand is very high. In Figure 5, the light blue line shows the maximum thermal production capacity of the power grid. The gray line represents the total load when there is a maximum penetration of EVs, compared to the orange line showing the demand without EVs. The blue line shows the wind power output. Figure 5 shows that for time interval 18 the load cannot be fully covered by the thermal production, represented by the yellow line, but the wind production is vital towards meeting the increased load. At the same hour, we can see that the committed thermal capacity is below the maximum available, as some power capacity is needed for ancillary services, while some units might be unavailable for production due to problems or regular maintenance schedules. That leads to the conclusion, that in absence of smart charging scheduling techniques, it is possible to need additional thermal capacity to meet peak hours' demand in the future.

In power systems with high renewable energy production penetration, it is vital to absorb as much renewable energy as possible, to enhance the operation of such units and take the full potential of low carbon emitting units. The results of the wind curtailment in our power system show that flexible load from EVs can be beneficial for the operation of renewable sources and the environment when combined with smart-charging mechanisms or market signals to EVs holders or users.

Finally, it is important to investigate the percentage of increase in the energy cost per MWh, in respect with the of EVs penetration rate. Figure 6 helps us draw some conclusions about that, especially on the huge impact of random charging profile. Firstly, we can see that the increase when using the optimized charging profile does not exceed 1.1% in the 100% EVs penetration scenario, compared

Figure 4: Total operational cost (\$) of the deterministic model under different charging profiles for various electric vehicles penetration



Figure 5: Overview of thermal production capacity, production mix and demand evolution, considering 100% electric vehicles penetration, maximum load and random charging profile

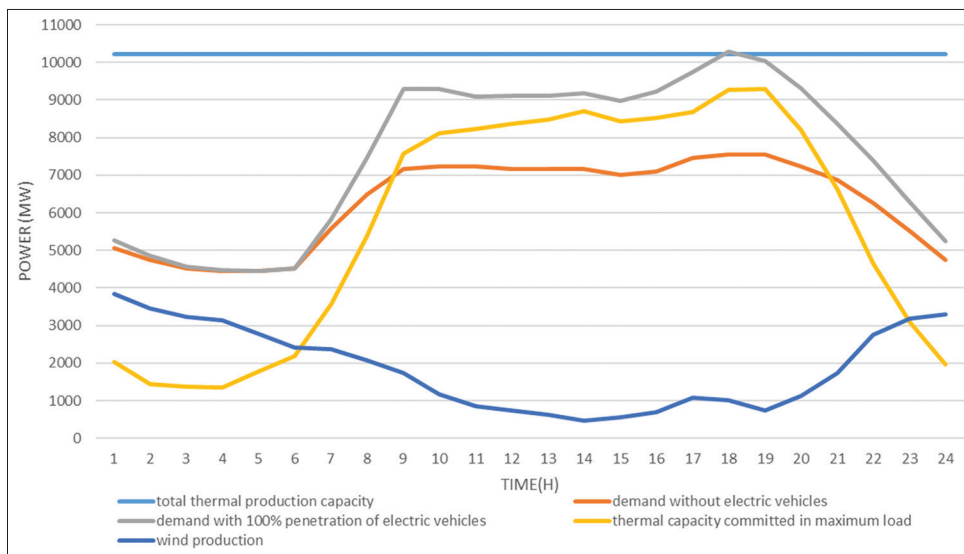
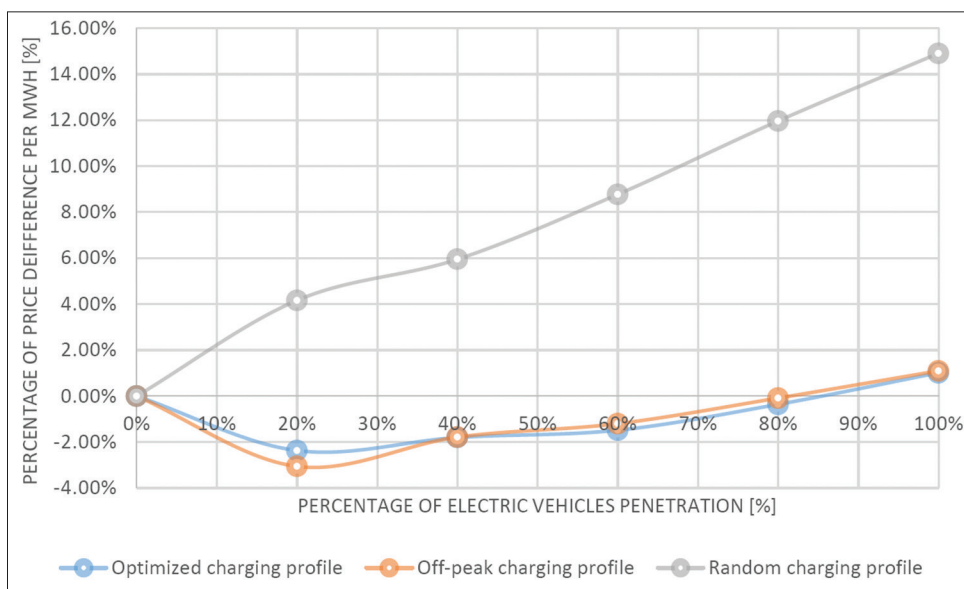


Figure 6: Percentage difference of the energy cost (\$/MWh) of the deterministic model solution based on 0% electric vehicles penetration energy cost



to no penetration of EVs. Secondly, in the random charging profile, we have a much higher increase which is growing faster after 40% of EVs penetration. That could be explained because after this certain percentage it will be mandatory to commit the most expensive units available. We also observe that there is a slight decrease of the price in the optimized charging profile and the off-peak hours charging profile. That has to do with the wind profile and the units committed. As we said before, we have used a non-favorable wind profile with high production during off-peak hours and low production during peak load hours. That leads to shutting down of many inflexible units during the off-peak hours and starting them up to meet peak loads. When we add the flexible load, it is distributed across those off-peak hours in a way that the system does not need to shut down units with high shut-down cost. That is the reason why the cost shows a slight decrease in small levels of penetration of EVs.

5.2. Stochastic Model Results

We have run the stochastic model for the same three charging scenarios, and we present the effect on the electricity demand in Annex V. The procedure to extract the data is the following: As long as we have ten different UC results, we multiply each result with the probability of the scenario. Similarly to the deterministic model, the results of the committed capacity when using charging profile 1 and 3 have minor differences. This conclusion comes out from both the load demand charts in Annex V and the total thermal production cost in Figure 7.

When using charging profile two, the maximum load in 100% EVs penetration exceed the total thermal production capacity slightly during hour 18 of the planning horizon. Wind power capacity helps the system to meet the increased load demand, although there should be an emergency plan in case of unexpected outages

in production units, such as demand response and interruptibility schemes. For the stochastic model, we have the same conclusion as for the deterministic model, concerning the evolution of the total operating cost, as shown in Figures 4 and 7.

The wind production curtailment results show us that the additional load from EVs can absorb some or all of the curtailed production especially when it is combined with an efficient charging method. However even when using the random charging profile, there is a slight decrease in the curtailed production. In any case, the curtailed production is a small percentage of the total demand, and we cannot lead to concrete conclusions, but there is an indication that excessive renewable energy can charge extra load from EVs.

The form of the curves for each charging profile for different EVs penetration is similar to those for the deterministic model. As the

number of EVs is increasing from 0% to nearly 80%, we observe that the cost for each MWh of energy produced is lower than in 0%, as shown in Figure 8. The explanation is that many expensive coal-fired units are used more efficiently while there is no need to shut them down during the low load hours and start them up again later when the load is higher. The avoidance of such startup and shut down costs is vital for the total production cost. However, we observe that in 100% penetration of EVs the percentage of increase of the cost is slightly higher than in the deterministic model for all the charging profiles. The conclusion from the above is that the model has a similar operation to the deterministic approach with a slightly higher operational cost, caused by the introduction of the stochastic nature of wind production.

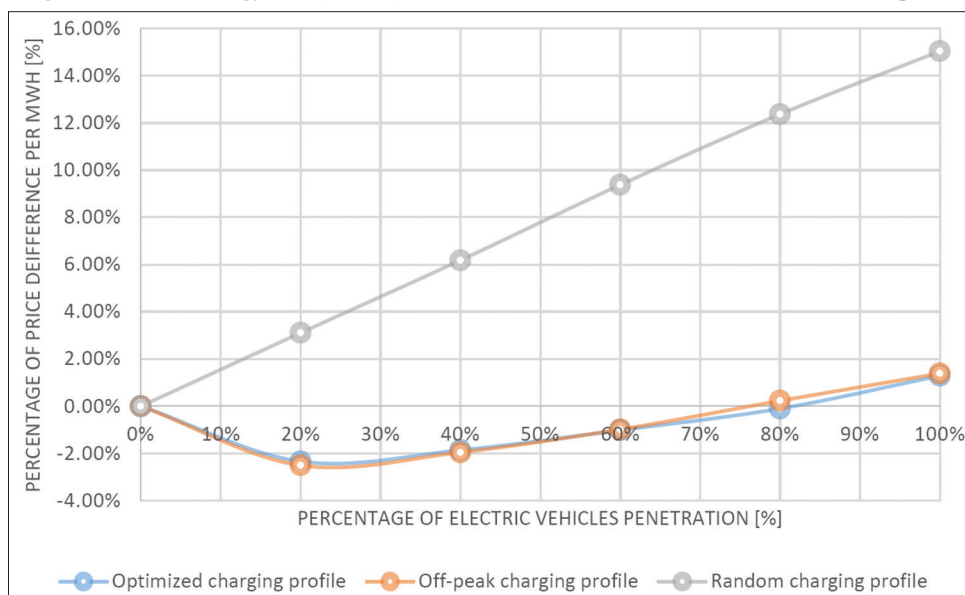
5.2.1. Interval unit model results

We have run the interval unit model for the same three charging scenarios, and we present the results in Annex V. First of all,

Figure 7: Total operational cost (\$) of the stochastic model under different charging profiles for various EVs penetration



Figure 8: Percentage difference of energy cost (\$/MWh) of the stochastic model solution based on 0% EVs penetration energy cost



we observe that the form of the load curves is different from the other two models. In this case, due to the higher robustness the algorithm distributes in a different way the flexible load than in the previous models. On the other hand, we observe that the resulted curves when using charging profile 1 and 3 are very similar, as in the previous models. The curves of the total operational cost, in Figure 9, have the same form as in the previous models. Specifically, the charging profile 1 and 3 have a similar cost, while profile 2 has a higher cost. However, the level of the total operational cost is significantly greater than in the previous models.

We have to mention that when using the random charging profile two, it is not possible to run the simulation in full (100%) EVs penetration, because the total production capacity is not enough to meet the demand. That is a major difference from the previous models. As we can see the system when using a higher robustness UC algorithm, the

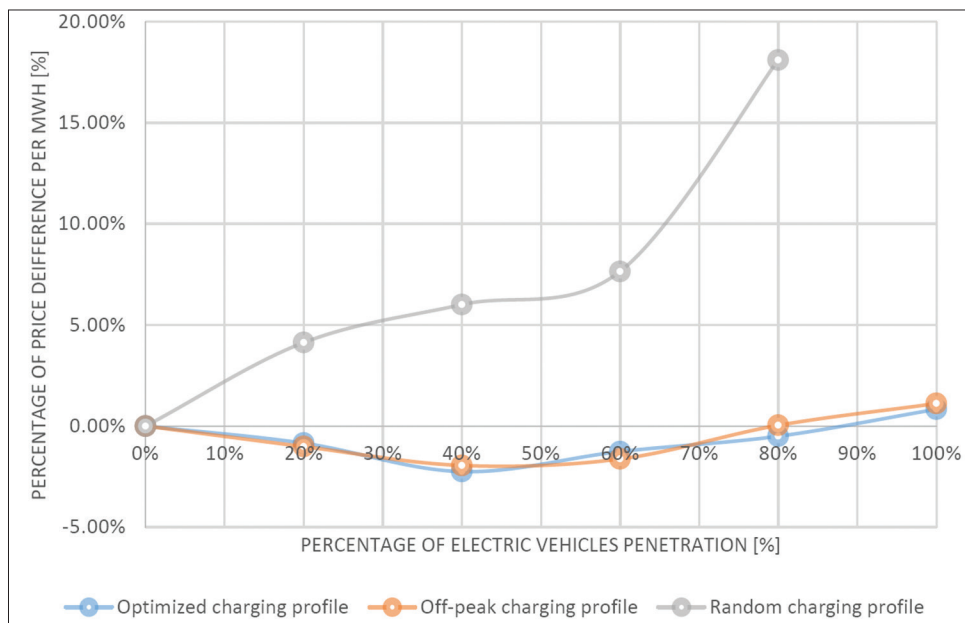
installed power plants are not able to provide enough electricity for the maximum number of EVs. This is more obvious in case of the fourth UC model the robust model. The curve for the random charging profile energy cost difference, in Figure 10, is smooth at the beginning until 60% of EVs penetration, and then it is very steep. That phenomenon can be explained by the higher unit capacity commitment of the interval model. As mentioned in section 2, the interval model commits more units to be able to cover extreme fluctuations of the wind power production, which means that for low levels of additional EVs load, the required capacity is already committed. However, for higher additional EVs loads, it commits the most expensive units.

The results of this model are quite different from the previous models. First of all, the available thermal production capacity was not enough to run the random charge profile for 100% of EVs penetration. Secondly, we have a higher total operational cost in

Figure 9: Total operational cost (\$) of the interval model solution under different charging profiles for various EVs penetration



Figure 10: Percentage difference of energy cost (\$/MWh) of the Interval model solution based on 0% EVs penetration energy cost



all cases due to higher reliability of the method. Thirdly, we have much more wind energy production curtailed which comes from the increased reliability of the solution produced.

5.3. Models Comparison

Finally, we are presenting a comparison, in Figures 11 and 12, between the three models regarding total operational cost, which reflects the total committed unit's capacity. The results for the deterministic model is the base, on which we are calculating the percentage differences between the deterministic and each of the other two models (stochastic and interval).

The comparison shows that the deterministic model is the cheapest one as it commits the capacity needed for the most probable

(deterministic) scenario. The stochastic scenario is slightly more expensive than the deterministic, as it introduces ten scenarios of wind production. Finally, the interval model is the most expensive, taking into account that it is the most robust compared to the others. Table 5 provides the performance ranking of the different UC models based on the total operational cost, for the different scenarios examined related to the penetration level of EVs (in %) and the charging profile. The represented percentages show the % increase of the total operational cost from the deterministic model.

The comparison between the UC models in Table 5, show that the most RUC model leads to higher total operating cost, due to its more conservative methodology to tackle the stochastic nature of wind. Moreover, from the above analysis, we derive

Figure 11: Comparison between the Stochastic model and the Deterministic model total operational cost

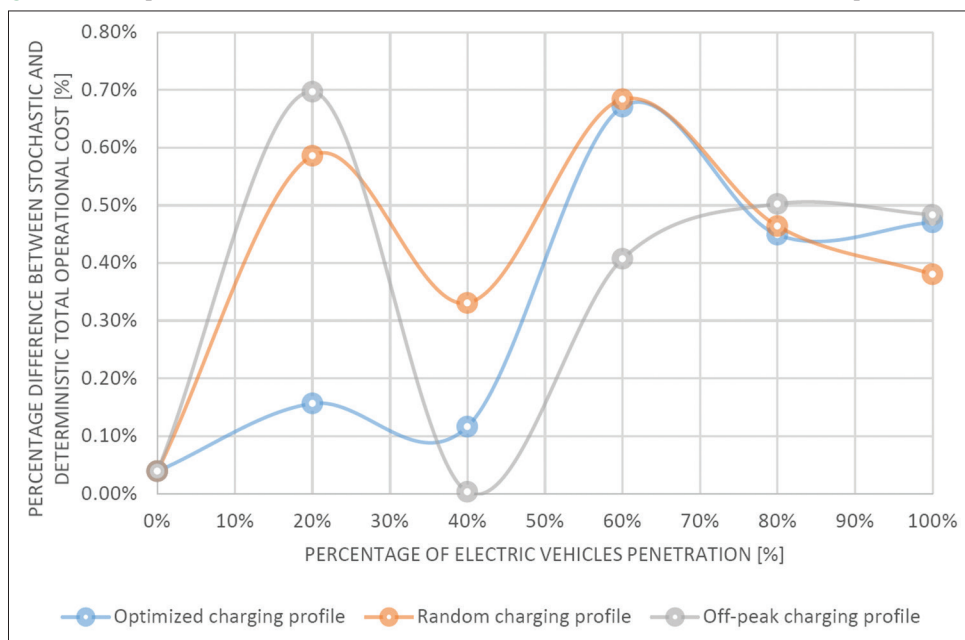


Figure 12: Comparison between the Interval model and the Deterministic model total operational cost

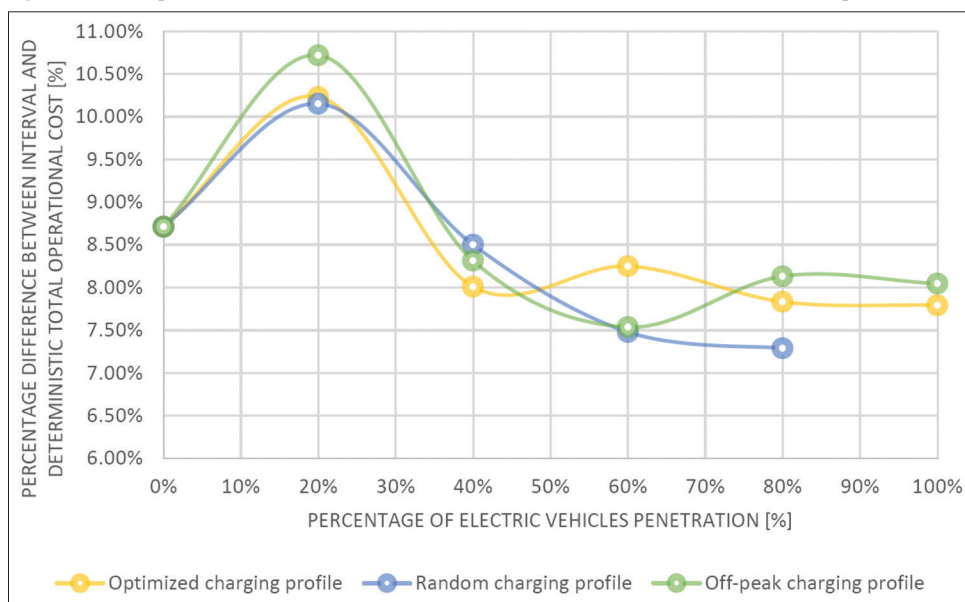


Table 5: Performance ranking of the UC models, based on the total operational cost, for the different EVs penetration level and charging profiles scenarios

| EVs Penetration (%) | Performance ranking | Profile 1 (optimized) | Profile 2 (random) | Profile 3 (off-peak) |
|---------------------|---------------------|-----------------------|---------------------|----------------------|
| 0% | 1 | Deterministic | | |
| | 2 | Stochastic (+0.04%) | | |
| | 3 | Interval (+8.71%) | | |
| 20% | 1 | Deterministic | Deterministic | Deterministic |
| | 2 | Stochastic (0.16%) | Stochastic (+0.59%) | Stochastic (+0.70%) |
| | 3 | Interval (+10.23%) | Interval (+10.15%) | Interval (+10.72%) |
| 40% | 1 | Deterministic | Deterministic | Deterministic |
| | 2 | Stochastic (0.12%) | Stochastic (+0.33%) | Stochastic (0%) |
| | 3 | Interval (+8.01%) | Interval (+8.50%) | Interval (+8.31%) |
| 60% | 1 | Deterministic | Deterministic | Deterministic |
| | 2 | Stochastic (0.67%) | Stochastic (+0.68%) | Stochastic (+0.41%) |
| | 3 | Interval (+8.25%) | Interval (+7.48%) | Interval (+7.54%) |
| 80% | 1 | Deterministic | Deterministic | Deterministic |
| | 2 | Stochastic (0.45%) | Stochastic (+0.46%) | Stochastic (+0.50%) |
| | 3 | Interval (+7.83%) | Interval (+7.29%) | Interval (+8.13%) |
| 100% | 1 | Deterministic | Deterministic | Deterministic |
| | 2 | Stochastic (0.47%) | Stochastic (+0.38%) | Stochastic (+0.8%) |
| | 3 | Interval (+7.79%) | -unable to run- | Interval (+8.05%) |

that the deterministic and the stochastic models allocate the EVs load in a similar way whereas the interval model allocates it in a different way. That can be explained by the fact that interval model handles the uncertainty of the wind production differently. The similarity of the stochastic and deterministic model is coming from the procedure used to create the deterministic scenario of wind production. The data that were used are the same, and the scenarios were extracted by using certain scenarios reduction methods. As a result, when combining the ten most probable scenarios into one then the outcome should be very close to the one most likely scenario (deterministic).

6. CONCLUSIONS

The integration of EVs in the power system is a challenging issue for the power system and network operators. The paper uses applies different mixed-integer linear programming UC models, which apply different methodologies to incorporate high levels of renewable energy production. The UC models, applying different methods to integrate the uncertainty from the renewables, are further extended to integrate the EVs, aiming to compare the UC models but as well the different charging profiles of the EVs. Our focus is on the effects of the excessive EVs’ load on the production side, hence the total operational cost, the average energy cost, the wind curtailment, the dispatch of power units, as well as the power grid adequacy to handle the extra load under different charging strategies and.

The selected power system is IEEE RTS 96 and the penetration levels of EVs vary from 0% to 100% with 20% steps. For the simulations, we used two charging strategies and a third one for confirmation. The first charging profile is a centrally controlled optimized profile, in which the UC algorithm selects the hours that will be allocating the excess load, to minimize the total production cost. The second charging profile is used to stress the power system and check the penetration levels of EVs that the system is ready to incorporate. The charging under the second strategy is done right after each vehicle’s trip and until is fully charged. The third

charging strategy was an off-peak hour charging profile, in which the EVs could be charged only during hours 1–8 and 21–24.

Simulation results show that an optimized charging strategy is considerably more efficient than the random charging strategy, both in the total operating cost and in the ability to integrate more EVs. The average cost of energy for the optimized charging for 100% of EVs penetration is not increasing more than 1.5% compared to the cost of energy for 0% EVs penetration. On the other hand, for the random charging strategy, the equivalent cost increases up to 15% for the same conditions. Furthermore, the advantage of using an optimized charging is the ability to integrate more EVs, which was challenged applying the most RUC model (interval). In that case, the model was not able to run for the 100% penetration due to lack of production capacity. Finally, the third charging profile gave us similar results with the optimized charging profile.

The comparison between the UC models confirmed our theoretical assumptions, that the most RUC model provides higher total operating cost, due to its more conservative approach to tackle uncertain renewable electricity generation. The results show, that the most robust model (interval) gives an average 8.5% more expensive solution than the less robust model. However, the middle robustness model (stochastic) solution is only 0.36% more expensive than the solution of the deterministic model. There exist a non-linear trade-off between power system robustness and total operating cost for the integration of EVs, depending on the characteristics of each power system, affecting also the penetration level of EVs.

The above conclusions could be further enhanced by further extensions or scenarios examined by the UC models. Such scenarios could consider more types of renewable sources, such as photovoltaics and biomass, or to consider a higher number of EVs or other types of chargers. Such model improvements could be the examination of further technologies as well as the usage of vehicle-to-grid technologies. Additionally, there could be

further improvements on the driving patterns. The patterns that were used are the same for the whole system. However such a big system might include different mix of cities and villages, where people certainly have different driving patterns. The application of detailed models are always very useful for decision making and for provision of insights on the expected impacts of the penetration of EVs. However, the spatial characteristics of each power system, the power capacity mix, the demand patterns, the available resources, as well as the structure of the regional economy and society – so as to capture potential driving patterns shifts and the penetration potential of different technologies-, are very important factors to be considered, in order to implement applications useful for real system and network operators.

REFERENCES

- André, M., Hammarström, U. (2000), Driving speeds in Europe for pollutant emissions estimation. *Transportation Research Part D: Transport and Environment*, 5(5), 321-335.
- Baringo, L., Amaro, R.S. (2017), A stochastic robust optimization approach for the bidding strategy of an electric vehicle aggregator. *Electric Power Systems Research*, 146, 362-370.
- Bertsimas, D., Litvinov, E., Sun, X.A., Zhao, J., Zheng, T. (2013), Adaptive robust optimization for the security constrained unit commitment problem. *IEEE Transactions on Power Systems*, 28(1), 52-63.
- Bharati, G.R., Paudyal, S. (2016), Coordinated control of distribution grid and electric vehicle loads. *Electric Power Systems Research*, 140, 761-768.
- Boumis, T. (2012), Energy Management of Electric Vehicles, Developing a Game Theory Model, in Order to Provide Ancillary Services to Grid. Master Thesis, National Technical University of Athens.
- CIA, (2017), The World Factbook. Central Intelligence Agency. Available from: <https://www.cia.gov/library/publications/resources/the-world-factbook>. [Last accessed on 2018 Oct 05].
- CIGRE, (2015), Integration of Electric Vehicles in Electric Power Systems. Final Report CIGRE. C6.20.
- Clement-Nyns, K., Haesen, E., Driesen, J. (2009), The impact of charging plug-in hybrid electric vehicles on a residential distribution grid. *IEEE Transactions on Power Systems*, 25(1), 371-380.
- Dagoumas, A., Koltsaklis, N., Panapakidis, I. (2017), An integrated model for risk management in electricity trade. *Energy*, 124, 350-363.
- Dagoumas, A., Polemis, M. (2017), An integrated model for assessing electricity retailer's profitability with demand response. *Applied Energy*, 198, 49-64.
- Dagoumas, A.S., Koltsaklis, N.E. (2017), Price signal of tradable guarantees of origin for hedging risk of renewable energy sources investments. *International Journal of Energy Economics and Policy*, 7(4), 59-67.
- Dvorkin, Y., Pandžić, H., Ortega-Vazquez, M.A., Kirschen, D.S. (2015), A hybrid stochastic/interval approach to transmission-constrained unit commitment. *IEEE Transactions on Power Systems*, 30(2), 621-631.
- Eurostat, (2017), Motorisation Rate, Cars per 1 000 Inhabitants. Available from: <http://www.ec.europa.eu/eurostat/tgm/table.do?tab=table&init=1&plugin=1&language=en&pcode=tsdpc340>. [Last accessed on 2018 Oct 05].
- Grahn, P. (2013), Electric Vehicle Charging Impact on Load Profile. Stockholm: Royal KTH Institute of Technology.
- Hanemann, P., Behnert, M., Bruckner, T. (2017), Effects of electric vehicle charging strategies on the German power system. *Applied Energy*, 203, 608-622.
- Haque, A.N.M., Ibn Saif, A.U.N., Nguyen, P.H., Torbaghan, S.S. (2016), Exploration of dispatch model integrating wind generators and electric vehicles. *Applied Energy*, 183, 1441-1451.
- Heydarian-Forushani, E., Golshan, M.E.H., Shafie-Khah, M. (2016), Flexible interaction of plug-in electric vehicle parking lots for efficient wind integration. *Applied Energy*, 179, 338-349.
- Kampman, B., van Essen, H., Braat, W., Grünig, M., Kantamaneni, R., Gabel, E. (2011), Impacts of Electric Vehicles-Deliverable 5 Impact Analysis for Market Uptake Scenarios and Policy Implications. CE Delft, Final Report Publication Number: 11.4058.07.
- Karfopoulos, E., Hatziargyriou, N. (2017), Distributed coordination of electric vehicles for conforming to an energy schedule. *Electric Power Systems Research*, 151, 86-95.
- Kasten, P., Bracker, J., Haller, M., Purwanto, J. (2016), Electric Mobility in Europe-Future Impact on the Emissions and the Energy Systems. Final Report-Task 2, Specific Contract Under Framework Contract EEA/ACC/13/003.
- Kirschen, D. (2014), Variants of Stochastic Unit Commitment. Seattle, WA: University of Washington.
- Koltsaklis, N., Dagoumas, A., Panapakidis, I. (2017), Impact of the penetration of renewables on flexibility need. *Energy Policy*, 109, 360-369.
- Koltsaklis, N.E., Dagoumas, A.S. (2018), Transmission expansion and electricity trade: A case study of the Greek power system. *International Journal of Energy Economics and Policy*, 8(5), 64-71.
- Koltsaklis, N.E., Georgiadis, M.C. (2016), An integrated unit commitment model incorporating electric vehicles as a flexible and responsive load. *Computer Aided Chemical Engineering*, 38, 1075-1080.
- Madzharov, D., Delarue, E., D'haeseleer, W. (2014), Integrating electric vehicles as flexible load in unit commitment modelling. *Energy*, 65, 285-294.
- Mariasiu, F. (2012), Energy sources management and future automotive technologies: Environmental impacts. *International Journal of Energy Economics and Policy*, 2(4), 342-347.
- Mkahl, R., Nait-Sidi-Moh, A., Gaber, J., Wack, M. (2017), An optimal solution for charging management of electric vehicles fleets. *Electric Power Systems Research*, 146, 177-188.
- Pandzic, H., Dvorkin, Y., Qiu, T., Wang, Y., Kirschen, D. (2017), Unit Commitment Under Uncertainty-GAMS Models. Seattle, USA: Library of the Renewable Energy Analysis Lab (REAL), University of Washington. Available from: http://www.ee.washington.edu/research/real/gams_code.html. [Last accessed on 2018 Oct 05].
- Plugincars, (2017), Compare Electric Cars and Plug-in Hybrids by Features, Price, Range. Available from: <http://www.plugincars.com/cars>. [Last accessed on 2018 Oct 05].
- REAL, (2017), Renewable Energy Analysis Lab-Library. Available from: <http://www.2.ee.washington.edu/research/real/index.html>; http://www.gridoptics.org/fpgws14/files/workshop/Kirschen-SCUCVariantsSoftwareSession_GOWS_FY14.pdf. [Last accessed on 2018 Oct 05]; [Last accessed on 2018 May 05].
- Schill, W.P., Gerbaulet, C. (2015), Power System Impacts of Electric Vehicles in Germany: Charging with Coal or Renewables? DIW Discussion Paper No. 1442.
- SITCA, (2017), RES 2005-2006, The National Travel Survey. Swedish Institute for Transport and Communications Analysis. Available from: http://www.trafa.se/globalassets/sika/sika-statistik/ss_2007_19_eng.pdf. [Last accessed on 2018 Oct 05].
- Tafreshi, S.M.M., Ranjbarzadeh, H., Jafari, M., Khayyam, H. (2016), A probabilistic unit commitment model for optimal operation of plug-in electric vehicles in microgrid. *Renewable and Sustainable Energy Reviews*, 66, 934-947.
- Talebzadeh, E., Rashidinejad, M., Abdollahi, A. (2014), Evaluation of plug-in electric vehicles impact on cost-based unit commitment. *Journal of Power Sources*, 248, 545-552.
- Tomic, J., Kempton, W. (2007), Using fleets of electric-drive vehicles for

- grid support. *Journal of Power Sources*, 168(2), 459-468.
- Ul-Haq, A., Cecati, C., El-Saadany, E. (2018), Probabilistic modeling of electric vehicle charging pattern in a residential distribution network. *Electric Power Systems Research*, 157, 126-133.
- Villar, J., Salas, E., Campos, E.C. (2016), Combined penetration of wind and solar generation with plug-in electric vehicles. *Energy Procedia*, 106, 59-72.
- Wang, M., Mu, Y., Jia, H., Zeng, P., Sheng, W. (2015), An efficient power plant model of electric vehicles for unit commitment of large-scale wind farms. *Energy Procedia*, 75, 1059-1064.
- Willett, K., Jasna, T. (2005), Vehicle-to-grid power implementation: From stabilizing the grid to supporting large-scale renewable energy.

- Journal of Power Sources*, 144(1), 280-294.
- Yang, Z., Li, K., Niu, Q., Xue, Y. (2017), A comprehensive study of economic unit commitment of power systems integrating various renewable generations and plug-in electric vehicles. *Energy Conversion and Management*, 132, 460-481.
- Zhang, N., Hu, Z., Han, X., Zhang, J., Zhou, Y. (2015), A fuzzy chance-constrained program for unit commitment problem considering demand response, electric vehicle and wind power. *International Journal of Electrical Power and Energy Systems*, 65, 201-209.
- Zhou, B., Littler, T., Meegahapola, L., Zhang, H. (2016), Power system steady-state analysis with large-scale electric vehicle integration. *Energy*, 115, 289-302.

ANNEX

Annex I: Basic formulation of the REAL UC models

Nomenclature

A. Sets

- B = Index of generating unit cost curve segments, 1- B
- I = Index of generating units, 1- I
- J = Index of generating unit start-up cost, 1- J
- L = Index of transmission lines, 1- L
- S = Index of bus bars, 1- S
- T = Index of hours, 1- T

B. Parameters

- a_i = Fixed production cost of unit i (\$)
- B_{sm} = Admittance of transmission line between nodes s - m (S)
- $d_s(t)$ = Load demand at bus s (MW)
- g_i^{down} = Minimum downtime of unit i (h)
- g_i^{up} = Minimum up time of unit i (h)
- $g_i^{down,init}$ = Time that unit i has been down before $t=0$ (h)
- $g_i^{up,init}$ = Time that unit i has been up before $t=0$ (h)
- g_i^0 = Output of unit i at $t=0$ (MW)
- g_i^{max} = Rated capacity of unit i (MW)
- g_i^{min} = Minimum output of unit i (MW)
- $g_{i,b}^{max}$ = Capacity of segment b of the cost curve of unit i (MW)
- $g_{i,b}^{on-off}$ = On-off status of unit i at $t=0$, equal to 1 if $g_i^{up,init} > 0$, otherwise 0
- k_{ib} = Slope of the segment b of the cost curve of unit i (\$/MW)
- I_{sm}^{max} = Capacity of the transmission line between nodes s - m (MW)
- $L_i^{down,min}$ = Length of time that unit i has to be off at the start of the planning horizon (h)
- $L_i^{up,min}$ = Length of time that unit i has to be on at the start of the planning horizon (h)
- M = Large number used for linearization
- $ramp_i^{down}$ = Ramp-down limit of unit i (MW/h)
- $ramp_i^{up}$ = Ramp-up limit of unit i (MW/h)
- $suc_{i,j}^{cost}$ = Cost steps in start-up cost curve of unit i (\$)
- $suc_{i,j}^{lim}$ = Time steps in start-up cost curve of unit i (h)

C. Variables

- $C_i(t)$ = Operating cost of unit i at time t (\$)
- $count_i^{down}$ = Unit i downtime period counter
- $g_i(t)$ = Output power of unit i at time t (MW)
- $g_{ib}(t)$ = Output power of unit i on segment b at time t (MW)
- $suc_i(t)$ = Start-up cost of unit i at time t (\$)
- $w_{ij}(t)$ = Binary variable equal to 1 if unit i is started at time t after being out for j hours, otherwise 0
- $x_i(t)$ = Binary variable equal to 1 if unit i is producing at time t , otherwise 0
- $y_i(t)$ = Binary variable equal to 1 if unit i is started at the beginning of time t , otherwise 0
- $z_i(t)$ = Binary variable equal to 1 if unit i is shutdown at the beginning of time t , otherwise 0
- $\theta_s(t)$ = Voltage angle at bus s (rad)

Formulation

The aim is to minimize the total generation cost of the thermal power plants which is described in the following objective function (Dvorkin et al., 2015).

$$\sum_{t=1}^T \sum_{i=1}^I C_i(t) \quad (1)$$

Expressions (2) and (3) describe the binary logic. Specifically, expression (3) prohibits a unit starting up to be simultaneously shut down. Expression (2) implements the logic that if a unit is starting up at time t , it cannot be on at time $t-1$.

$$y_i(t) - z_i(t) = x_i(t) - x_i(t-1) \quad \forall 1 \leq t \leq T, i \leq I \quad (2)$$

$$y_i(t) + z_i(t) \leq 1 \quad \forall t \leq T, i \leq I \quad (3)$$

Equation (4) defines the total cost for each unit i . The total cost is the summation of the startup cost of the units (if needed), the fixed cost and the variable cost:

$$C_i(t) = \alpha \cdot x_i(t) + \sum_{b=1}^B kb \cdot g_{i,b}(t) + suc_i(t) \quad \forall t \leq T, i \leq I \quad (4)$$

The total unit output is equal to the sum of the generation in each segment of the cost curve:

$$g_i(t) = \sum_{b=1}^B g_{i,b}(t) \quad \forall t \leq T, i \leq I \quad (5)$$

Minimum unit output must be higher than the minimum output of unit i :

$$g_i(t) \geq g_i^{min} \cdot x_i(t) \forall t \leq T, i \leq I \tag{6}$$

Unit output for each generation level.

$$g_{i,b}(t) \geq g_{i,b}^{max} \cdot x_i(t) \forall t \leq T, i \leq I, b \leq B \tag{7}$$

Minimum up time constraints:

$$\sum_{t=1}^{L_i^{up,min}} (1 - x_i(t)) = 0 \forall i \leq I \tag{8}$$

$$\sum_{tt=t}^{t+g_i^{up}-1} x_i(tt) \geq g_i^{up} \cdot y_i(t) \forall L_i^{up,min} + 1 \leq t \leq T - g_i^{up} + 1, i \leq I \tag{9}$$

$$\sum_{tt=t}^T (x_i(tt) - y_i(t)) \geq 0 \forall T - g_i^{up} + 2 \leq t \leq T, i \leq I \tag{10}$$

Where $L_i^{up,min} = \max \{0, \min \{T, (g_i^{up} - g_i^{up,init}) \cdot g_i^{on-off}\} \}$

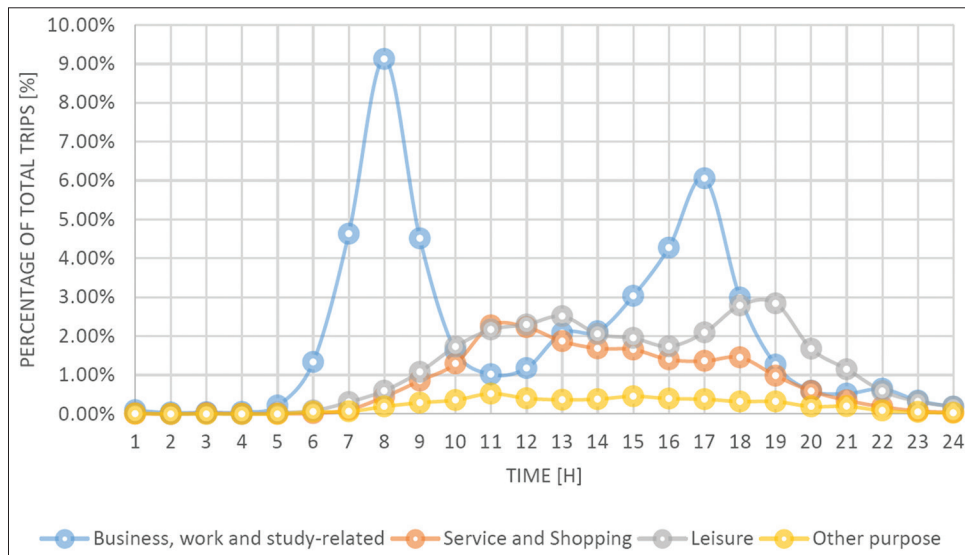
Minimum down time constraints:

$$\sum_{t=1}^{L_i^{down,min}} x_i(t) = 0 \forall i \leq I \tag{11}$$

Annex II Table 1: Trips that start withing each hour period categorized by purpose

| Hour | Business, work and study-related (%) | Service and shopping (%) | Leisure (%) | Other purpose (%) |
|------|--------------------------------------|--------------------------|-------------|-------------------|
| 1 | 0.09 | 0.01 | 0.03 | 0.01 |
| 2 | 0.03 | 0.00 | 0.00 | 0.00 |
| 3 | 0.04 | 0.02 | 0.01 | 0.00 |
| 4 | 0.05 | 0.01 | 0.00 | 0.00 |
| 5 | 0.21 | 0.01 | 0.03 | 0.00 |
| 6 | 1.33 | 0.02 | 0.08 | 0.05 |
| 7 | 4.63 | 0.11 | 0.30 | 0.06 |
| 8 | 9.12 | 0.44 | 0.60 | 0.19 |
| 9 | 4.51 | 0.85 | 1.08 | 0.29 |
| 10 | 1.62 | 1.29 | 1.73 | 0.35 |
| 11 | 1.02 | 2.27 | 2.17 | 0.52 |
| 12 | 1.18 | 2.23 | 2.30 | 0.40 |
| 13 | 2.08 | 1.87 | 2.51 | 0.36 |
| 14 | 2.12 | 1.68 | 2.05 | 0.38 |
| 15 | 3.04 | 1.65 | 1.95 | 0.45 |
| 16 | 4.27 | 1.40 | 1.74 | 0.39 |
| 17 | 6.06 | 1.36 | 2.09 | 0.38 |
| 18 | 2.99 | 1.45 | 2.79 | 0.32 |
| 19 | 1.26 | 0.98 | 2.84 | 0.32 |
| 20 | 0.60 | 0.59 | 1.68 | 0.19 |
| 21 | 0.52 | 0.35 | 1.15 | 0.20 |
| 22 | 0.64 | 0.18 | 0.59 | 0.08 |
| 23 | 0.34 | 0.08 | 0.32 | 0.05 |
| 24 | 0.18 | 0.04 | 0.18 | 0.02 |

Annex II Figure 1: Starting time of different category of trips over a 24-hour period



$$\sum_{t=t}^{t+g_i^{down}} (1-x_i(t)) \geq g_i^{down} \cdot z_i(t) \forall L_i^{down, min} + 1 \leq t \leq T - g_i^{down} + 1, i \leq I \tag{12}$$

$$\sum_{t=t}^T (1-x_i(t) - z_i(t)) \geq 0 \forall T - g_i^{down} + 2 \leq t \leq T, i \leq I \tag{13}$$

Where $L_i^{down, min} = \max \{0, \min \{T, (g_i^{down} - g_i^{down, init}) \cdot (1 - g_i^{on-off})\} \}$

Ramp-up and ramp-down constraints:

$$-ramp_i^{down} \leq g_i(t) - g_i(t-1) \forall 2 \leq t \leq T, i \leq I \tag{14}$$

$$ramp_i^{up} \geq g_i(t) - g_i(t-1) \forall 2 \leq t \leq T, i \leq I \tag{15}$$

$$-ramp_i^{down} \leq g_i(t_1) - g_i^o \forall i \leq I \tag{16}$$

$$ramp_i^{up} \geq g_i(t_1) - g_i^o \forall i \leq I \tag{17}$$

Expression (18) and equations (19) and (20) impose the constraints and calculate the startup cost of each unit i. Specifically, inequation (18) sets the limitations for the calculation of the value of variable $w_{ij}(t)$, taking into account the initial conditions.

$$w_{ij}(t) \leq \sum_{t=suc_{ij}^{lim}}^{\min \{t-1, suc_{i,j+1}^{lim}-1\}} z_i(t-j) + 1 \$ \{j \leq J - 1 \wedge suc_{i,j}^{lim} \leq g_i^{down, init} + t - 1 < suc_{i,j+1}^{lim}\} + 1 \$ \{j = J \wedge suc_{i,j}^{lim} \leq g_i^{down, init} + t - 1\} \forall t \leq T, i \leq I, j \leq J \tag{18}$$

$$\sum_{j=1}^J w_{ij}(t) = y_i(t) \forall t \leq T, i \leq I \tag{19}$$

$$suc_i(t) = \sum_{j=1}^J suc_{ij}^{cost} \cdot w_{ij}(t) \forall t \leq T, i \leq I \tag{20}$$

Where symbol \$ represents logical IF and symbol \$\wedge\$ symbolizes logical AND.

Equation (21) defines the power balance in the electrical system.

$$\sum_{i=1}^I g_i(t) - \sum_{\{s,m\} \in L | m > s} B_{sm} \cdot (\theta_s(t) - \theta_m(t)) - \sum_{\{s,m\} \in L | m < s} B_{sm} \cdot (\theta_m(t) - \theta_s(t)) \forall t \leq T, s \leq S \tag{21}$$

Transmission constraints:

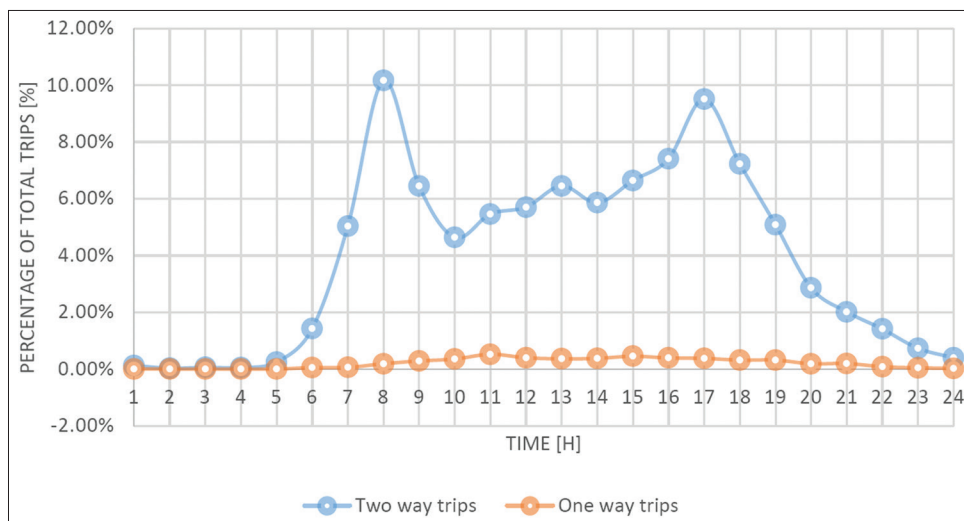
$$-l_{sm}^{max} \leq B_{sm} \cdot (\theta_s(t) - \theta_m(t)) \leq l_{sm}^{max} \forall t \leq T, \{s,m\} \in L \tag{22}$$

$$-\pi \leq \theta_s(t) \leq \pi \forall t \leq T, s \leq S \tag{23}$$

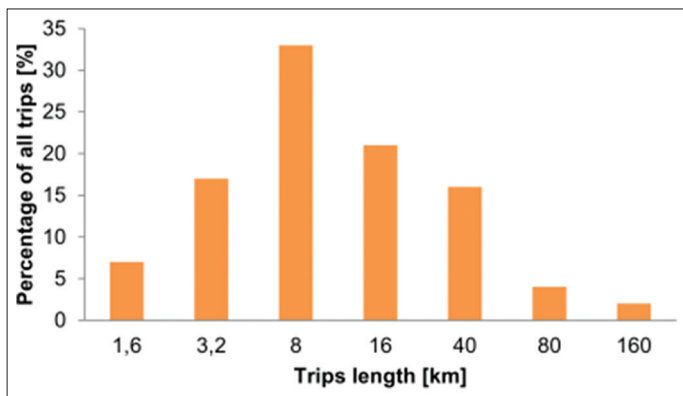
Annex II Table 2: Starting time of one-way and two-way trips over a 24 h period

| Hour | Two-way trips (%) | One way trips (%) |
|------|-------------------|-------------------|
| 1 | 0.13 | 0.01 |
| 2 | 0.03 | 0.00 |
| 3 | 0.06 | 0.00 |
| 4 | 0.05 | 0.00 |
| 5 | 0.25 | 0.00 |
| 6 | 1.43 | 0.05 |
| 7 | 5.04 | 0.06 |
| 8 | 10.16 | 0.19 |
| 9 | 6.44 | 0.29 |
| 10 | 4.64 | 0.35 |
| 11 | 5.46 | 0.52 |
| 12 | 5.70 | 0.40 |
| 13 | 6.45 | 0.36 |
| 14 | 5.86 | 0.38 |
| 15 | 6.64 | 0.45 |
| 16 | 7.41 | 0.39 |
| 17 | 9.51 | 0.38 |
| 18 | 7.23 | 0.32 |
| 19 | 5.08 | 0.32 |
| 20 | 2.86 | 0.19 |
| 21 | 2.02 | 0.20 |
| 22 | 1.41 | 0.08 |
| 23 | 0.73 | 0.05 |
| 24 | 0.40 | 0.02 |

Annex II Figure 2: Starting time of one-way and two-way trips over a 24-hour period



Annex II Figure 3: Percentage of trips in each Trip length group



Source: Madzharov, et al., 2014

Annex II Table 3: Average speed for each of the length groups

| Tri type | Trip length (km) | Average speed (km/h) |
|-----------------|------------------|----------------------|
| Urban roads | 1.6 | 26 |
| Urban roads | 3.2 | 26 |
| Urban roads | 8 | 26 |
| Urban roads | 16 | 26 |
| Secondary roads | 40 | 44 |
| Main roads | 80 | 86 |
| Motor ways | 160 | 115 |

Source: Andréa and Hammarströmb, 2000

Annex III Table 1: Trips (t.e.s): The trips that start each hour for each group of EVs(e) for each bus bar (s)

| Trips (t.e.s) | | s101 | s102 | s103 |
|---------------|----|----------|----------|----------|
| t6 | e1 | 130.4002 | 130.4002 | 130.4002 |
| t6 | e2 | 304.2671 | 304.2671 | 304.2671 |
| t6 | e3 | 588.6119 | 588.6119 | 588.6119 |
| t6 | e4 | 376.7116 | 376.7116 | 376.7116 |
| t6 | e5 | 291.5893 | 291.5893 | 291.5893 |
| t6 | e6 | 72.4445 | 72.4445 | 72.4445 |

Annex III Table 2: EVsAvailable (t.e.s): The EVs that are parked and available for charging

| EVsAvailable (t.e.s) | | s101 | s102 | s103 |
|----------------------|----|----------|----------|----------|
| t1 | e1 | 4533.78 | 4533.78 | 4533.78 |
| t1 | e2 | 10578.82 | 10578.82 | 10578.82 |
| t1 | e3 | 20464.98 | 20464.98 | 20464.98 |
| t1 | e4 | 13097.59 | 13097.59 | 13097.59 |
| t1 | e5 | 10138.04 | 10138.04 | 10138.04 |
| t1 | e6 | 2518.77 | 2518.77 | 2518.77 |

$$\theta_s(t) = 0 \quad \forall t \leq T \tag{24}$$

Annex II. Driving patterns

The main goal of the model is to reproduce in a realistic way the driving patterns of real life. Therefore, we should process the statistical data from national authorities that are available. According to the Swedish Institute for Transport and Communication Analysis, which had made an extensive survey of Swedish resident’s traveling patterns during the period 1/10/2005 and 30/9/2006, the car is the most common means of transport (SITCA, 2017). In this paper, the journeys are separated into four

Annex III Table 3: Consumption(e): The EVs consumption in MWh according to their distance group

| Consumption(e) | Column1 |
|----------------|---------|
| e1 | 0.00028 |
| e2 | 0.00056 |
| e3 | 0.00140 |
| e4 | 0.00280 |
| e5 | 0.00700 |
| e6 | 0.01400 |
| e7 | 0.02800 |

Annex III Table 4: BatteryFull(e): The total capacity of the batteries of EVs in each distance group (e) in (MWh)

| BatteryFull(e) | Column1 |
|-----------------|----------|
| e1 | 11583.81 |
| e2 | 27028.89 |
| e3 | 52288.03 |
| e4 | 33464.34 |
| e5 | 25902.69 |
| e6 | 6435.45 |
| e7 | 4183.04 |

Annex III Table 5: ChargeLine(e): The power of the charger that each group of EVs is mounted on in MW

| ChargeLine(e) | Column1 |
|---------------|---------|
| e1 | 0.003 |
| e2 | 0.003 |
| e3 | 0.003 |
| e4 | 0.003 |
| e5 | 0.003 |
| e6 | 0.003 |
| e7 | 0.006 |

Annex III Table 6: MaxTransfer (t.e.s): The maximum power that could be ejected from the power system for charging the EVs at each hour

| MaxTransfer (t.e.s) | | s101 | s102 | s103 |
|---------------------|----|----------|----------|----------|
| t1 | e1 | 13.60134 | 13.60134 | 13.60134 |
| t1 | e2 | 31.73647 | 31.73647 | 31.73647 |
| t1 | e3 | 61.39495 | 61.39495 | 61.39495 |
| t1 | e4 | 39.29277 | 39.29277 | 39.29277 |
| t1 | e5 | 30.41411 | 30.41411 | 30.41411 |
| t1 | e6 | 7.55630 | 7.55630 | 7.55630 |

broad categories. Business, work, and study -related; Service and shopping; Leisure; Other purpose.

For each one of the categories above, it is measured how many journeys start during each hour. To be able to use the statistics we make the following assumptions:

1. The statistics regard journeys with any transport. Therefore, we assume that the same rates apply to car transportation also.
2. The statistics are based on periods of 60 minutes. For convenience reasons, in the model building, we assume that all the journeys start at the end of each period.
3. We assume that trips from categories 1, 2 and 3 are two-way travel, whereas category four journeys are one-way trips.

Annex II Tables 1 and 2 and Annex II Figure 1, based on the above analysis, provide the Trips that start within each hour period categorized by purpose and the Starting time of different category of trips over a 24-h period respectively.

Annex II Figure 1 shows that journeys from categories 1-3 from two peaks in a way that confirms our assumption that they are two-way trips. The logic behind that is that someone leaves his/her house in the morning and returns later. For example, we observe that work-related journeys peak at 08.00 and then at 17.00 which is a typical schedule for workers. Furthermore, half of the journeys happen until 14.00 and the other half is made after that time. Helping us to understand the two-way trips better. For that reason, we aggregate the journeys for the first three categories into one category called two-way journeys and those from the fourth category to one-way trips, shown in Annex II Table 2 and Annex II Figure 2.

Annex II Figure 3 shows the distribution of trip lengths that will be used for the calculations.

The average speed used in this research is presented in Annex II Table 3, from which it is derived. That every trip starting in a period will travel for less than an hour and therefore, in an ideal situation it will be charging during the next period. That

happens for all the length groups except the longest ones which are the smaller by percentage group.

In the UC models' input file, we add the following parameters, shown in Annex III Tables 1-6.

Annex II Figure 1 shows that journeys from categories 1, 2 and 3 from two peaks in a way that confirms our assumption that they are two-way trips. The logic behind that is that someone leaves his/her house in the morning and returns later. For example, we observe that work-related journeys peak at 08.00 and then at 17.00 which is a typical schedule for workers. Furthermore, half of the journeys happen until 14.00, and the other half is made after that time, helping us to understand the two-way trips better. For that reason, we aggregate the journeys for the first three categories into one category called two-way journeys and those from the fourth category to one-way trips, shown in Annex II Table 2 and Annex II Figure 2.

The average speed used in this research is presented in Annex II Table 3, from which it is derived. That every trip starting in a period will travel for less than an hour and therefore, in an ideal situation it will be charging during the next period. That happens for all the length groups except the longest ones which are the smaller by percentage group.